JOURNAL OF THE ROYAL SOCIETY Interface

Tuning the geometrical parameters of biomimetic fibrillar structures to enhance adhesion

Shaohua Chen and Ai Kah Soh

J. R. Soc. Interface 2008 **5**, 373-383
doi: 10.1098/rsif.2007.1121

JOURNAL OF THE ROYAL SOCIETY Interface

J. R. Soc. Interface (2008) **5**, 373–382
doi:10.1098/rsif.2007.1121
Published online 17 July 2007

Tuning the geometrical parameters of biomimetic fibrillar structures to enhance adhesion

Shaohua Chen[1,*] and Ai Kah Soh[2]

[1]*LNM, Institute of Mechanics, Chinese Academy of Sciences, Beijing 100080, China*
[2]*Department of Mechanical Engineering, The University of Hong Kong, Hong Kong, China*

Fibrillar structures are common features on the feet of many animals, such as geckos, spiders and flies. Theoretical analyses often use periodical array to simulate the assembly, and each fibril is assumed to be of equal load sharing (ELS). On the other hand, studies on a single fibril show that the adhesive interface is flaw insensitive when the size of the fibril is not larger than a critical one. In this paper, the Dugdale–Barenblatt model has been used to study the conditions of ELS and how to enhance adhesion by tuning the geometrical parameters in fibrillar structures. Different configurations in an array of fibres are considered, such as line array, square and hexagonal patterns. It is found that in order to satisfy flaw-insensitivity and ELS conditions, the number of fibrils and the pull-off force of the fibrillar interface depend significantly on the fibre separation, the interface interacting energy, the effective range of cohesive interaction and the radius of fibrils. Proper tuning of the geometrical parameters will enhance the pull-off force of the fibrillar structures. This study may suggest possible methods to design strong adhesion devices for engineering applications.

Keywords: adhesion; fibrillar interface; contact mechanics; pull-off force

1. INTRODUCTION

The attachment systems in jumping spiders and geckos are believed to rely entirely on van der Waals forces between the finely structured feet and substrates (Autumn *et al.* 2000, 2002; Russell 2002; Kesel *et al.* 2003). Of particular significance are the many fibrils on the feet of these animals. Fibrillar structure is an important feature of these adhesion systems.

Owing to the reliance on van der Waals forces, the ability of geckos to adhere to substrates is primarily controlled by mechanics rather than surface chemistry. Hence, the geometry and material properties of the structure must play a pivotal role in enhancing the adhesion (Gorb & Scherge 2000; Niederegger *et al.* 2002; Geim *et al.* 2003; Gao *et al.* 2005; Huber *et al.* 2005; Spolenak *et al.* 2005; Yao & Gao 2006; Chen & Gao 2007). Various mechanical models have been developed to model specific hairy attachment systems (e.g. Hui *et al.* 2002; Persson 2003; Glassmaker *et al.* 2004; Hui *et al.* 2004) within the framework of adhesive contact mechanics (e.g. Johnson *et al.* 1971; Derjaguin *et al.* 1975; Roberts & Thomas 1975; Muller *et al.* 1980; Greenwood & Johnson 1981; Barquins 1988; Maugis 1992; Carpick *et al.* 1996; Chaudhury *et al.* 1996; Baney & Hui 1997; Johnson & Greenwood 1997; Barthel 1998; Greenwood & Johnson 1998; Kim *et al.* 1998; Robbe-Valloire & Barquins 1998; Morrow *et al.* 2003; Schwarz 2003; Chen & Wang 2006). In particular, the Johnson–Kendall–Roberts (JKR) model (Johnson *et al.* 1971) of contact mechanics has been used to show that splitting of a single contact into multiple smaller contacts always results in enhanced adhesion strength (Autumn *et al.* 2002; Arzt *et al.* 2003), and developed to explain the other adhesion problems in biology (Chen & Gao 2006*a–c*). One of the puzzling predictions of the JKR-type model is that the spatula structure of geckos can be split ad infinitum to support arbitrarily large body weights. This is clearly impossible as the adhesion strength cannot exceed the theoretical strength of van der Waals interaction (Gao *et al.* 2005; Tang *et al.* 2005). In order to explain why the characteristic size of the fibrillar ultrastructure of bioattachment systems falls in a narrow range between a few hundred nanometres and a few micrometres and the optimal conditions under which the theoretical pull-off force can be achieved, Gao & Yao (2004) found that the robust design of shape-insensitive optimal adhesion becomes possible only when the diameter of the fibre is reduced to length scales of the order of 100 nm and the optimal adhesion could be achieved by a combination of size reduction and shape optimization. The smaller the size, the less important the shape. In order to simulate the fibrillar structure, Glassmaker *et al.* (2004) and Hui *et al.* (2004) studied the concept of equal load sharing (ELS) for a perfect interface containing many fibrils and presented results on how a fibrillar structure enhances adhesion.

*Author for correspondence (chenshaohua72@hotmail.com).

Received 25 May 2007
Accepted 24 June 2007

In real life, most surfaces are actually rough, and surface roughness has been considered in many contact literatures. Meine *et al.* (2004) did experiments to find a correlation between the contact area and adhesion of rough surfaces, and the roughness was simulated by a structure. A simple method of using the JKR model to determine the interfacial adhesion between two ideal rough surfaces was demonstrated by Hodges *et al.* (2004) for individual asperity–asperity and asperity–flat contacts. ELS was also adopted by Hodges *et al.* (2004). An analytical model based on the JKR theory of adhesion was used by Hui *et al.* (2001) to study the contact mechanics and adhesion of a periodically rough surface.

In order to be convenient in studying the adhesion force or adhesion strength, most people have assumed that the fibrillar structure or the asperity of a rough surface is periodical and the force is homogeneously distributed on all the asperities or fibres, i.e.

$$P = NF, \tag{1.1}$$

where P is the pull-off force; N is the number of the asperities or fibres; and F is the pull-off force for single asperity or fibril contact.

Whether the pull-off force on each asperity or fibre attains the same value homogeneously and simultaneously (flaw insensitivity) was not investigated in the mentioned literatures. Are there any restrictions on the geometrical parameters to attain flaw insensitivity and satisfy ELS in fibrillar structures? The concept of flaw insensitivity has been adopted to understand the mechanics of biological systems (Gao *et al.* 2003; Persson 2003; Gao & Yao 2004; Glassmaker *et al.* 2004; Hui *et al.* 2004; Gao & Chen 2005; Gao 2006). In the state of flaw insensitivity, pre-existing crack-like flaw does not propagate or participate in the failure process so that the biological material failure occurs by uniform rupture at the limiting strength of the material. Examples are as follows.

The spatula in a gecko's attachment system was modelled by Gao *et al.* (2005) as an elastic cylinder with a flat tip in adhesive contact with a rigid substrate. The radius of the cylinder is R and the actual contact radius is $a = \alpha R$, where $0 < \alpha \leq 1$. The rim of $\alpha R < r < R$ represents flaws or regions of poor adhesion. Gao *et al.* (2005) used the Griffith criterion and obtained the critical size of the radius of the cylinder as

$$R_{\mathrm{cr}} = \beta^2 \frac{\Delta\gamma E^*}{\sigma_{\mathrm{th}}^2}, \tag{1.2}$$

at which the traction within the contact area uniformly reaches the theoretical strength σ_{th} and the pull-off force becomes $P = \sigma_{\mathrm{th}} \pi a^2$. In the above equation, $\beta = \sqrt{2/\pi\alpha F_1^2}$, where $F_1(\alpha)$ is a function varying in a narrow range between 0.4 and 0.5 for $0 \leq \alpha \leq 0.8$; $E^* = E/(1-\nu^2)$, where E and ν are the Young modulus and the Poisson ratio of the cylinder, respectively; and $\Delta\gamma$ is the van der Waals interaction energy.

If we let $\alpha = 1$, the critical radius of the cylinder becomes

$$R_{\mathrm{cr}} = \frac{8}{\pi} \frac{\Delta\gamma E^*}{\sigma_{\mathrm{th}}^2}, \tag{1.3}$$

which is identical to the result obtained by Persson (2003), where a rigid circular disc with radius R on a flat substrate with Young's modulus E and Poisson's ratio ν has been studied. Persson (2003) assumed that complete contact occurs at the interface and found that if $R \leq R_{\mathrm{cr}}$, then the bond breaking may occur uniformly over the contact area and the pull-off stress is then independent of the size R and reaches the theoretical interface strength σ_{th}.

In this paper, the concept of ELS for a perfect interface containing many fibrils will be studied. All fibrils have radius not larger than the critical size of flaw insensitivity of a single fibre. The plan of this paper is as follows. We first study the problem of two-dimensional fibrillar structure, and then three-dimensional one. In the two-dimensional case, we first discuss the critical size of the fibril, the pull-off force and the pull-off stress required to pull off a single fibril under the condition of flaw insensitivity, and then use a plane-strain fibrillar interface model to study the restrictions on the number of fibrils and how to enhance the pull-off force. In the three-dimensional models, the corresponding aspects considered in the two-dimensional models will be investigated for different fibrillar distributing patterns, such as line array, square and hexagonal lattices.

2. PLANE-STRAIN MODELS

Adhesive contact between elastic objects usually fails by the propagation of crack-like flaws initiated at poor contact regions around surface asperities, impurities, trapped contaminants, etc. Under this circumstance, the adhesion strength is not optimal because it is only a small fraction of material theoretical strength. From the robustness point of view, it would be best to design a material that allows the contact to fail not by crack propagation but by uniform detachment at the theoretical strength of adhesion, which is called flaw tolerance (Gao *et al.* 2003, 2005; Gao & Chen 2005) or flaw insensitivity (Glassmaker *et al.* 2004; Hui *et al.* 2004).

Inspired by the concept of flaw insensitivity, in this paper, we will assume that the fibrils with size not larger than the critical one are under ELS and the interface strength between each fibril and the substrate attains the theoretical strength. Thus, using the boundary condition that the maximum separation at the interface should not be larger than the effective interaction distance of the interface, we can obtain the relations between the various geometrical parameters, the pull-off force and the pull-off stress for different fibrillar configurations.

2.1. Critical size of a single fibril

Figure 1 shows a plane-strain model, in which a rigid plate with width $2h$ contacts an elastic substrate with Young's modulus E and Poisson's ratio ν. Perfect adhesion is assumed as that in Persson (2003) and the contact half-width is h. The Dugdale model will be used to obtain the critical half-width h_{cr} required by the condition of flaw insensitivity. When $h \leq h_{\mathrm{cr}}$, the tractions on the interface will uniformly attain the interface

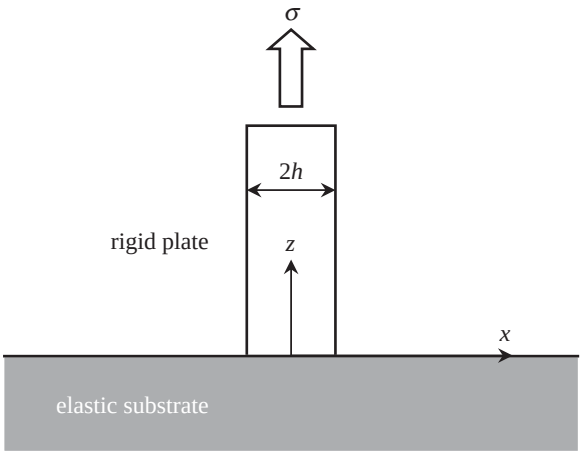

Figure 1. Plane-strain model for pulling a rigid plate from an elastic substrate to find a critical size of the plate h_{cr}, under which the interface tractions will attain homogeneously the theoretical interface strength σ_{th} at pull-off.

theoretical strength σ_{th}. The pulling stress is denoted by σ on the upper boundary, as shown in figure 1.

From the solution of a two-dimensional elastic half-space pulled by a homogeneous traction σ within the length region $2h$, the normal displacement can be expressed as (Johnson 1985)

$$u_z(x) = \frac{-\sigma}{\pi E^*}\left\{(h+x)\ln\left(\frac{h+x}{h}\right)^2 + (h-x)\ln\left(\frac{h-x}{h}\right)^2\right\} + C, \tag{2.1}$$

where C is an arbitrary constant.

The cohesive law in the Dugdale–Barenblatt model (Dugdale 1960; Barenblatt 1985) can be expressed as

$$\sigma(\delta) = \begin{cases} \sigma_{th} & \delta(x) \le \delta_0 \\ 0 & \delta(x) > \delta_0 \end{cases}, \tag{2.2}$$

where $\sigma(\delta) = \sigma$ is the normal traction on the adhesion interface; δ_0 is the effective range of cohesive interaction; and $\delta(x)$ is the separation between the two surfaces of the contact interface. The interfacial energy is

$$\Delta\gamma = \sigma_{th}\delta_0. \tag{2.3}$$

Consider the flaw insensitive concept. At the moment of pull-off, the maximum opening displacement at the contact edge should not be larger than the effective interaction range δ_0, i.e. $\delta(h) \le \delta_0$. Thus, the normal traction on the adhesion interface $\sigma = \sigma(\delta)$ uniformly attains the interfacial theoretical strength σ_{th}. The critical size h_{cr} of the above rigid plate can be obtained from

$$\delta(h_{cr}) = \delta_0, \tag{2.4}$$

where

$$\delta(h) = u_z(0) - u_z(h). \tag{2.5}$$

Substituting equation (2.1) into the critical criterion (2.4) yields

$$h_{cr} = \frac{\pi E^* \delta_0}{2\sigma_{th}\ln 4} \quad E^* = \frac{E}{1-\nu^2}. \tag{2.6}$$

When $h \le h_{cr}$, the pull-off stress is the theoretical strength σ_{th} and has no relation to the width of the rigid plate.

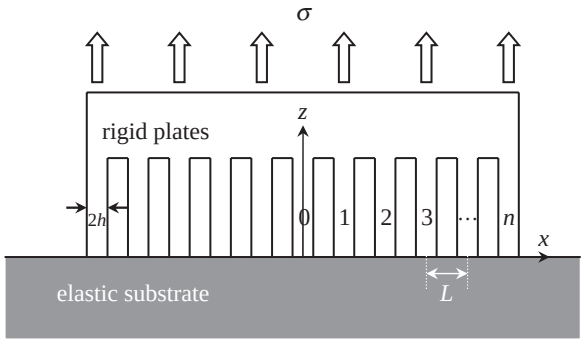

Figure 2. Schematic of an idealized scenario where a large number of identical rigid plates are in perfect contact with an elastic substrate. All the plates with half-width $h \le h_{cr}$ are subjected to the same external loading σ and the interface tractions are homogeneous theoretical interface strength σ_{th}.

The corresponding pull-off force F_p is

$$F_p = 2\sigma_{th}h. \tag{2.7}$$

2.2. *Fibrillar structure*

Hui *et al.* (2004) and Glassmaker *et al.* (2004) have studied the concept of ELS for a perfect interface containing many fibrils, in which they used the area fraction that fibrils cover and found enhanced adhesion compared with their non-fibrillar counterparts. Are there any other limits on the number of fibres to satisfy the condition of ELS in the regime of flaw insensitivity except for the characteristic fibril spacing that prevents fibrils' self-matting? How can we enhance adhesion by tuning the geometrical parameters?

A simple plane-strain fibrillar structure in adhesive contact with a substrate is shown in figure 2. The fibrils in figure 2 are assumed to be rigid and identical in width $2h \le 2h_{cr}$ and ELS in this section, which would be valid, for example, if the structure in the figure is pulled uniformly upwards. The distance between neighbouring fibres is L. There are $N = 2n+1$ fibrils consisting of the fibrillar interface with the central one numbered '0' in figure 2.

Inspired by Hui *et al.* (2004), if the fibrils are elastic with Young's modulus E_f and length l, the energy per unit length in the direction of thickness needed to pull off a single fibril is

$$2h\left(\frac{\sigma_{th}^2 l}{2E_f} + \Delta\gamma\right). \tag{2.8}$$

The work required to detach a unit area of the interface is

$$\left(\frac{\sigma_{th}^2 l}{2E_f} + \Delta\gamma\right)\rho, \tag{2.9}$$

where $\rho = (2n+1)h/(nL+h)$ is the area fraction that the fibres cover on the interface.

ELS and theoretical strength conditions have been satisfied above. One should note that another condition of flaw insensitivity is that the maximum separation of the interface should not be larger than the effective interaction range δ_0, which will lead to restrictions on the number of fibrils N.

Consider the model in figure 2, in which the fibrils are rigid. The normal displacement $u_z(x)$ at an arbitrary point $(x, 0)$ consists of the contributions of

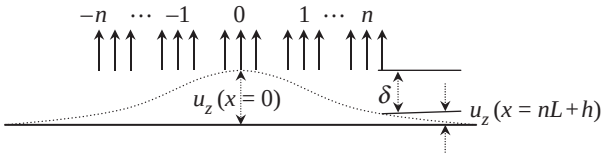

Figure 3. Schematic of the deformation of an elastic half-plane under uniformly distributing tractions. The maximum separation is denoted by δ.

all the distributing tractions on the interface, and each part can be obtained from equation (2.1) as follows. For example,

$$u_{z0}=\frac{-\sigma_{\mathrm{th}}}{\pi E^*}\left\{(h+x)\ln\left(\frac{h+x}{h}\right)^2+(h-x)\ln\left(\frac{h-x}{h}\right)^2\right\}+C_0, \tag{2.10}$$

denotes the displacement at the point $(x, 0)$ contributed by the zeroth distributing traction, where C_0 is a constant.

$$u_{z1}=\frac{-\sigma_{\mathrm{th}}}{\pi E^*}\left\{(h+x-L)\ln\left(\frac{h+x-L}{h}\right)^2+(h-x+L)\ln\left(\frac{h-x+L}{h}\right)^2\right\}+C_1, \tag{2.11}$$

denotes the displacement at the point $(x, 0)$ contributed by the first distributing traction.

$$u_{zi}=\frac{-\sigma_{\mathrm{th}}}{\pi E^*}\left\{(h+x-iL)\ln\left(\frac{h+x-iL}{h}\right)^2+(h-x+iL)\ln\left(\frac{h-x+iL}{h}\right)^2\right\}+C_i, \tag{2.12}$$

denotes the displacement at the point $(x, 0)$ contributed by the ith ($i=\pm1,\pm2,\ldots,\pm n$) distributing traction.

The total displacement at the point $(x, 0)$ can be written as

$$\begin{aligned}u_z(x)&=u_{z0}+u_{z1}+\cdots+u_{zn}+u_{z(-1)}+\cdots+u_{z(-n)}\\&=\frac{-\sigma_{\mathrm{th}}}{\pi E^*}\left\{(h+x)\ln\left(\frac{h+x}{h}\right)^2+(h-x)\ln\left(\frac{h-x}{h}\right)^2\right\}\\&\quad+\sum_{n=1}^{N}\frac{-\sigma_{\mathrm{th}}}{\pi E^*}\left\{(h+x-nL)\ln\left(\frac{h+x-nL}{h}\right)^2+(h-x+nL)\ln\left(\frac{h-x+nL}{h}\right)^2\right\}\\&\quad+\sum_{n=1}^{N}\frac{-\sigma_{\mathrm{th}}}{\pi E^*}\left\{(h+x+nL)\ln\left(\frac{h+x+nL}{h}\right)^2+(h-x-nL)\ln\left(\frac{h-x-nL}{h}\right)^2\right\}+C,\end{aligned} \tag{2.13}$$

where $C=C_0+C_1+\cdots+C_n+C_{-1}+\cdots+C_{-n}$.

Note the model in figure 3. The maximum separation δ can be written as

$$\delta(nL+h)=u_z(0)-u_z(nL+h). \tag{2.14}$$

Substituting equation (2.13) into (2.14) yields

$$\begin{aligned}&\delta(nL+h)\\&=\sum_{i=1}^{n}\frac{-\sigma_{\mathrm{th}}h}{\pi E^*}\left\{\left(1-i\frac{L}{h}\right)\ln\left(1-i\frac{L}{h}\right)^2+\left(1+i\frac{L}{h}\right)\ln\left(1+i\frac{L}{h}\right)^2\right\}\\&\quad+\sum_{i=1}^{n}\frac{-\sigma_{\mathrm{th}}h}{\pi E^*}\left\{\left(1+i\frac{L}{h}\right)\ln\left(1+i\frac{L}{h}\right)^2+\left(1-i\frac{L}{h}\right)\ln\left(1-i\frac{L}{h}\right)^2\right\}\\&\quad+\frac{\sigma_{\mathrm{th}}h}{\pi E^*}\left\{\left(2+n\frac{L}{h}\right)\ln\left(2+n\frac{L}{h}\right)^2-n\frac{L}{h}\ln\left(n\frac{L}{h}\right)^2\right\}\\&\quad+\sum_{i=1}^{n}\frac{\sigma_{\mathrm{th}}h}{\pi E^*}\left\{\left[2+(n-i)\frac{L}{h}\right]\ln\left(2+(n-i)\frac{L}{h}\right)^2\right.\\&\quad\left.+(-n+i)\frac{L}{h}\ln\left((-n+i)\frac{L}{h}\right)^2\right\}\\&\quad+\sum_{i=1}^{n}\frac{\sigma_{\mathrm{th}}h}{\pi E^*}\left\{\left[2+(n+i)\frac{L}{h}\right]\ln\left(2+(n+i)\frac{L}{h}\right)^2\right.\\&\quad\left.-(n+i)\frac{L}{h}\ln\left((n+i)\frac{L}{h}\right)^2\right\}.\end{aligned} \tag{2.15}$$

Flaw insensitivity requires

$$\delta(nL+h)\le\delta_0. \tag{2.16}$$

The critical case $\delta(nL+h)=\delta_0$ yields the relation between the non-dimensional parameter L/h and the critical number $N=2n+1$, which is dependent only on the non-dimensional parameter $\sigma_{\mathrm{th}}h/E^*\delta_0$.

The pull-off stress σ_{p} and the pull-off force F_{p} per unit length in the direction of thickness are

$$\frac{\sigma_{\mathrm{p}}}{\sigma_{\mathrm{th}}}=\rho,\quad\frac{F_{\mathrm{p}}}{2h\sigma_{\mathrm{th}}}=N,\quad\rho=\frac{N}{nL/h+1}. \tag{2.17}$$

From the above, one can see that the normalized pull-off stress and pull-off force are identical to the area fraction and the number of fibrils, respectively.

3. THREE-DIMENSIONAL MODELS

Three-dimensional models of fibrillar adhesive interface will be studied in this section. The anti-bunching condition for fibres of square cross-section in fibrillar structures has been investigated by Hui *et al.* (2002) and Gao *et al.* (2005). Glassmaker *et al.* (2004) have derived the critical length for bunching of cylindrical fibres. Owing to rigid fibrils considered in this paper, anti-bunching condition was not investigated in our model.

3.1. Critical size of a single fibril

A rigid cylindrical fibre with radius R in contact with an elastic substrate is shown in figure 4, which was analysed by Persson (2003) with energy method and Hui *et al.* (2004) with Maugis' (1992) solution. The contact zone is assumed to be perfect adhesion with contact radius R. If the bond break is flaw insensitive, then the pull-off stress should be the theoretical strength σ_{th}; thus the tractions on the interface are also σ_{th}.

The normal displacement at any point of a three-dimensional elastic half-space subjected to homogeneous pulling stress σ_{th} in an area with radius R can

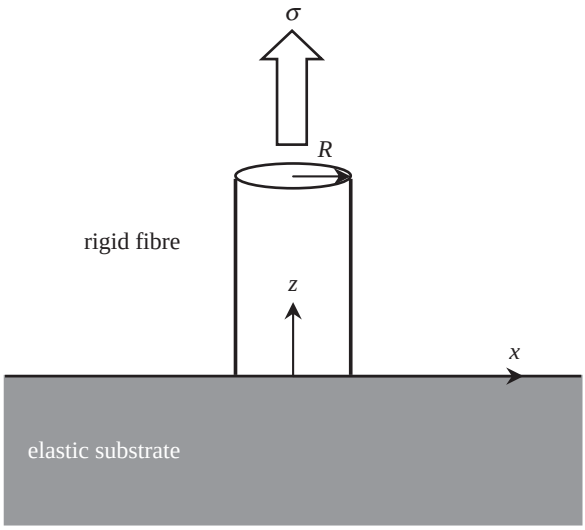

Figure 4. Pull-off of a rigid fibril from an elastic substrate. The adhesion is assumed to be perfect to find a critical radius R_{cr}, under which the interface traction attains the theoretical interface strength at pull-off.

be obtained from Johnson (1985) as

$$u_z(r) = \frac{4\sigma_{th}R}{\pi E^*} P\left(\frac{r}{R}\right), \quad r < R \tag{3.1}$$

and

$$u_z(r) = \frac{4\sigma_{th}r}{\pi E^*}\left\{P\left(\frac{R}{r}\right) - \left(1-\frac{R^2}{r^2}\right)K\left(\frac{R}{r}\right)\right\}, \quad r > R, \tag{3.2}$$

where the functions are

$$P(R/r) = \int_0^{(\pi/2)} \left\{1-(R^2/r^2)\sin^2\varphi\right\}^{1/2} \mathrm{d}\varphi \tag{3.3}$$

and

$$K(R/r) = \int_0^{(\pi/2)} \left\{1-(R^2/r^2)\sin^2\varphi\right\}^{-1/2} \mathrm{d}\varphi. \tag{3.4}$$

The maximum separation δ can be obtained,

$$\delta(R) = u_z(0) - u_z(R) \tag{3.5}$$

where

$$u_z(0) = \frac{2\sigma_{th}R}{E^*} \qquad u_z(R) = \frac{4\sigma_{th}R}{\pi E^*}. \tag{3.6}$$

Then we have

$$\delta(R) = \frac{4\sigma_{th}R}{\pi E^*}\left(\frac{\pi}{2}-1\right). \tag{3.7}$$

Flaw-insensitivity condition requires

$$\delta(R) \le \delta_0. \tag{3.8}$$

The critical contact radius can be derived from $\delta(R) = \delta_0$ as

$$R_{cr} = \frac{\pi E^* \Delta\gamma}{4(\pi/2-1)\sigma_{th}^2}, \tag{3.9}$$

which means that if $R \le R_{cr}$, then the bond breaking may occur uniformly over the contact area and the pull-off stress is then independent of the size R of the cylinder.

The corresponding pull-off force is given by

$$F_p = \pi\sigma_{th}R^2. \tag{3.10}$$

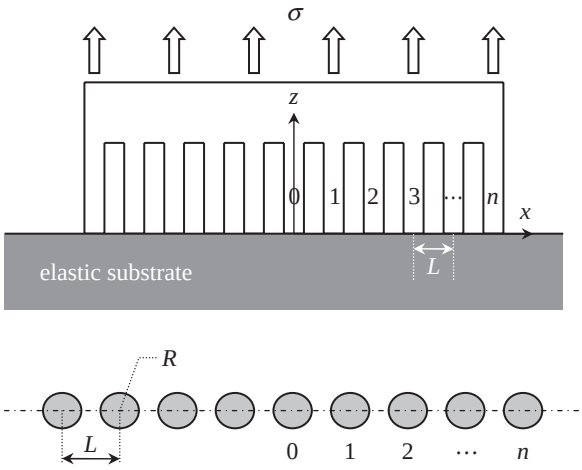

Figure 5. Schematic of a large number of identical rigid and cylindrical fibrils which are in perfect contact with an elastic substrate. Each fibril has radius $R \le R_{cr}$, and the interface tractions between each fibril and substrate are assumed to be homogeneous theoretical interface strength at pull-off to find the constraints on the number of fibrils.

The critical size in equation (3.9) is identical to that in Hui *et al.* (2004). Comparing equations (3.9) and (1.3), one can find that the critical size predicted by the Dugdale criterion is more conservative than that predicted by the Griffith criterion, which is similar to the flaw-insensitivity conditions for a thin strip with a central crack or double-edge cracks in Gao & Chen (2005).

3.2. Fibres distributed in a line array

We consider a fibrillar structure consisting of a line array of fibres as shown in figure 5, where a large number of identical fibrils are in perfect contact with an elastic substrate. We assume that the fibrils are rigid with radius $R \le R_{cr}$ and the distance between neighbouring fibrils is L. The contact region is assumed to be a rectangular area with width $2R$ and length $2(nL+R)$.

When a uniformly distributing stress acts to pull the fibrillar structure as shown in figure 5, we know that under the ELS and flaw-insensitivity assumptions the normal traction on the interface is the theoretical strength σ_{th}. The normal displacement at the point $x=0$ can be obtained from Johnson (1985) as

$$u_{z0} = \frac{4\sigma_{th}R}{\pi E^*}P(0) + 2\sum_{i=1}^{n}\frac{4\sigma_{th}iL}{\pi E^*}\{P(R/iL) - (1-R^2/(iL)^2)K(R/iL)\}. \tag{3.11}$$

The normal displacement at the point $x = nL + R$ is

$$u_{zn} = \frac{4\sigma_{th}R}{\pi E^*}P(1) + \sum_{i=1}^{2n}\frac{4\sigma_{th}(iL+R)}{\pi E^*}\{P[R/(iL+R)] - [1-R^2/(iL+R)^2]K[R/(iL+R)]\}. \tag{3.12}$$

Thus, the maximum separation of the fibrillar interface at the contact edge,

$$\delta = u_{z0} - u_{zn} \le \delta_0, \tag{3.13}$$

should not be larger than δ_0, i.e. $\delta \le \delta_0$. $\delta = \delta_0$ denotes the critical case. For a given h and L, the constraint relation

between the number of fibres $N=2n+1$ and the non-dimensional parameter $\sigma_{\mathrm{th}}R/E^*\delta_0$ can be described.

The pull-off force and pull-off stress can then be written as

$$\frac{F_{\mathrm{p}}}{\pi\sigma_{\mathrm{th}}R^2}=N,\quad \frac{\sigma_{\mathrm{p}}}{\sigma_{\mathrm{th}}}=\rho,\quad \rho=\frac{\pi}{4}\frac{N}{(nL/R+1)}, \tag{3.14}$$

where ρ is the area fraction of the fibrillar interface in a line array pattern.

3.3. Fibres distributed in a hexagonal pattern

Figure 6 shows a hexagonal distributing pattern for a fibrillar structure, in which fibres with radius $R\le R_{\mathrm{cr}}$ are assumed to be rigid and the substrate is an elastic half-space. ELS and flaw insensitivity are assumed in this model and the contact area is a circular region with radius $nL+R$.

The normal displacement at the centre point $r=0$ can be written as

$$\begin{aligned}u_{z0}=&\frac{4\sigma_{\mathrm{th}}R}{\pi E^*}P(0)\\&+6\sum_{i=1}^{n}\frac{4\sigma_{\mathrm{th}}iL}{\pi E^*}\{P(R/iL)-[1-R^2/(iL)^2]K(R/iL)\}\\&+6\sum_{n_2=1}^{n_1-1}\sum_{n_1=2}^{n}\frac{4\sigma_{\mathrm{th}}r_1}{\pi E^*}\{P(R/r_1)-(1-R^2/r_1^2)K(R/r_1)\},\end{aligned} \tag{3.15}$$

where

$$r_1=\sqrt{(n_1L)^2+(n_2L)^2-2n_1n_2L^2\cos\frac{\pi}{3}}. \tag{3.16}$$

The corresponding displacement at $r=nL+R$ is approximately written as

$$\begin{aligned}u_{zn}=&\frac{4\sigma_{\mathrm{th}}R}{\pi E^*}P(1)+\sum_{i=1}^{2n}\frac{4\sigma_{\mathrm{th}}(iL+R)}{\pi E^*}\{P[R/(iL+R)]\\&-[1-R^2/(iL+R)^2]K[R/(iL+R)]\}\\&+2\sum_{n_2=0}^{n}\sum_{n_1=1}^{n}\frac{4\sigma_{\mathrm{th}}r_2}{\pi E^*}\{P(R/r_2)-[1-R^2/r_2^2]K(R/r_2)\}\\&+2\sum_{n_2=n+1}^{2n-n_1}\sum_{n_1=1}^{n-1}\frac{4\sigma_{\mathrm{th}}r_2}{\pi E^*}\{P(R/r_2)-(1-R^2/r_2^2)K(R/r_2)\},\end{aligned} \tag{3.17}$$

where

$$r_2=\sqrt{(n_1L)^2+(n_2L)^2-2n_1n_2L^2\cos\frac{2\pi}{3}}. \tag{3.18}$$

The maximum separation at the contact edge can be obtained as

$$\delta=u_{z0}-u_{zn}. \tag{3.19}$$

The critical condition of flaw insensitivity for the fibrillar interface is

$$\delta=\delta_0. \tag{3.20}$$

The above equation shows that the relation between the normalized parameter L/R and the number of fibrils N depends only on the non-dimensional parameter $\sigma_{\mathrm{th}}R/E^*\delta_0$. The number of fibres is

$$N=6n+1+6\sum_{i=1}^{n-1}i. \tag{3.21}$$

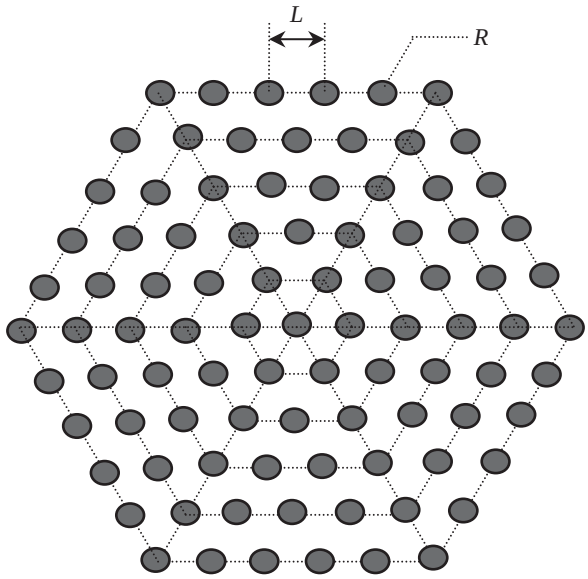

Figure 6. The fibrillar structure with rigid cylindrical fibres distributed in hexagonal lattice patterns.

The pull-off force F_{p} and pull-off stress σ_{p} in this case can be expressed as

$$\frac{F_{\mathrm{p}}}{\pi\sigma_{\mathrm{th}}R^2}=N,\quad \frac{\sigma_{\mathrm{p}}}{\sigma_{\mathrm{th}}}=\rho,\quad \rho=N\left(\frac{1}{nL/R+1}\right)^2. \tag{3.22}$$

3.4. Fibres distributed in square pattern

Figure 7 shows the square distribution pattern of a fibrillar interface, in which rigid fibrils are assumed with distance L between neighbouring fibres. The contact region between the fibrillar structure and the substrate is a circular one with radius $nL+R$.

The normal displacement at $x=0$ can be expressed as (Johnson 1985)

$$\begin{aligned}u_{z0}=&\frac{4\sigma_{\mathrm{th}}R}{\pi E^*}P(0)+4\sum_{i=1}^{n}\frac{4\sigma_{\mathrm{th}}iL}{\pi E^*}\{P(R/iL)\\&-[1-R^2/(iL)^2]K(R/iL)\}\\&+4\sum_{n_2=1}^{\mathrm{int}\sqrt{n^2-n_1^2}}\sum_{n_1=1}^{n}\frac{4\sigma_{\mathrm{th}}r_1}{\pi E^*}\{P(R/r_1)-(1-R^2/r_1^2)K(R/r_1)\}.\end{aligned} \tag{3.23}$$

The corresponding displacement at $x=nL+R$ is

$$\begin{aligned}u_{zn}=&\frac{4\sigma_{\mathrm{th}}R}{\pi E^*}P(1)+\sum_{i=1}^{2n}\frac{4\sigma_{\mathrm{th}}(iL+R)}{\pi E^*}\{P[R/(iL+R)]\\&-[1-R^2/(iL+R)^2]K[R/(iL+R)]\}\\&+2\sum_{i=1}^{n}\frac{4\sigma_{\mathrm{th}}r_2}{\pi E^*}\{P(R/r_2)-[1-R^2/r_2^2]K(R/r_2)\}\\&+2\sum_{n_2=1}^{\mathrm{int}\sqrt{n^2-n_1^2}}\sum_{n_1=1}^{n}\frac{4\sigma_{\mathrm{th}}r_3}{\pi E^*}\{P(R/r_3)-(1-R^2/r_3^2)K(R/r_3)\}\\&+2\sum_{n_2=1}^{\mathrm{int}\sqrt{n^2-n_1^2}}\sum_{n_1=1}^{n}\frac{4\sigma_{\mathrm{th}}r_4}{\pi E^*}\{P(R/r_4)-(1-R^2/r_4^2)K(R/r_4)\},\end{aligned} \tag{3.24}$$

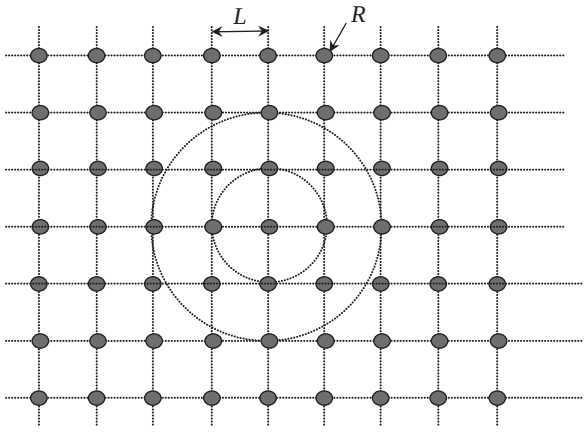

Figure 7. The fibrillar structure with rigid cylindrical fibres distributed in square lattice patterns.

where

$$r_1 = \sqrt{(n_1 L)^2 + (n_2 L)^2}, \tag{3.25}$$

$$r_2 = \sqrt{(nL + R)^2 + (iL)^2}, \tag{3.26}$$

$$r_3 = \sqrt{(nL + R + n_1 L)^2 + (n_2 L)^2} \tag{3.27}$$

and

$$r_4 = \sqrt{(nL + R - n_1 L)^2 + (n_2 L)^2}. \tag{3.28}$$

The maximum normal separation can be obtained as

$$\delta = u_{z0} - u_{zn}, \tag{3.29}$$

which satisfies the flaw-insensitivity condition

$$\delta \leq \delta_0. \tag{3.30}$$

$\delta = \delta_0$ denotes the critical case from which one can find the relation between the normalized parameter L/R and the number of all fibres N depending only on the non-dimensional parameter $\sigma_{\mathrm{th}} R/E^* \delta_0$. The critical number of fibrils N that satisfies ELS and flaw-insensitivity conditions is

$$N = 1 + 4n + 4 \sum_{n_1=1}^{n} \mathrm{int} \sqrt{n^2 - n_1^2}. \tag{3.31}$$

The pull-off force F_{p} and pull-off stress σ_{p} can be expressed by N and ρ, respectively, as

$$\frac{F_{\mathrm{p}}}{\pi \sigma_{\mathrm{th}} R^2} = N, \quad \frac{\sigma_{\mathrm{p}}}{\sigma_{\mathrm{th}}} = \rho, \quad \rho = N \left(\frac{1}{nL/R + 1} \right)^2, \tag{3.32}$$

where ρ is the area fraction of fibres in a square lattice pattern.

4. NUMERICAL ANALYSIS

4.1. Two-dimensional fibrillar interface contact

In the plane-strain model of a rigid plate in contact with an elastic half-plane, the normalized pull-off force is equal to the critical number of fibres, which can be found in equation (2.17). Figure 8*a* shows the normalized pull-off force and the critical number of plates N as a function of the normalized space L/h to satisfy ELS and flaw sensitivity conditions for different values of non-dimensional parameter $\sigma_{\mathrm{th}} h/E^* \delta_0$, from which one can see that the pull-off force remains almost a constant for a determined parameter $\sigma_{\mathrm{th}} h/E^* \delta_0$ when the space L/h increases. It means that the size of the plane-strain fibrillar structure can be very large and does not influence the pull-off force when the ELS and flaw sensitivity are satisfied and the half-width of each plate h is not larger than the critical size h_{cr}. On the other hand, for a determined space L/h of the fibrillar structure, increase in the net pull-off force can only be realized through decreasing $\sigma_{\mathrm{th}} h/E^* \delta_0$, i.e. by increasing the effective Young's modulus of the substrate E^* or the effective interaction distance δ_0. In addition, for a fixed space L/h, a larger critical number N can be expected by means of increasing the value of δ_0 and E^* or decreasing σ_{th}. According to equation (2.17), one can see that the normalized effective strength (pull-off stress) $\sigma_{\mathrm{p}}/\sigma_{\mathrm{th}}$ and the area fraction ρ will decrease along with an increasing space L/h as shown in figure 8*b*. It should be of interest to design plane-strain fibrillar structures as adhesion-controlled devices, whose size or pull-off force can be regulated according to the requirements.

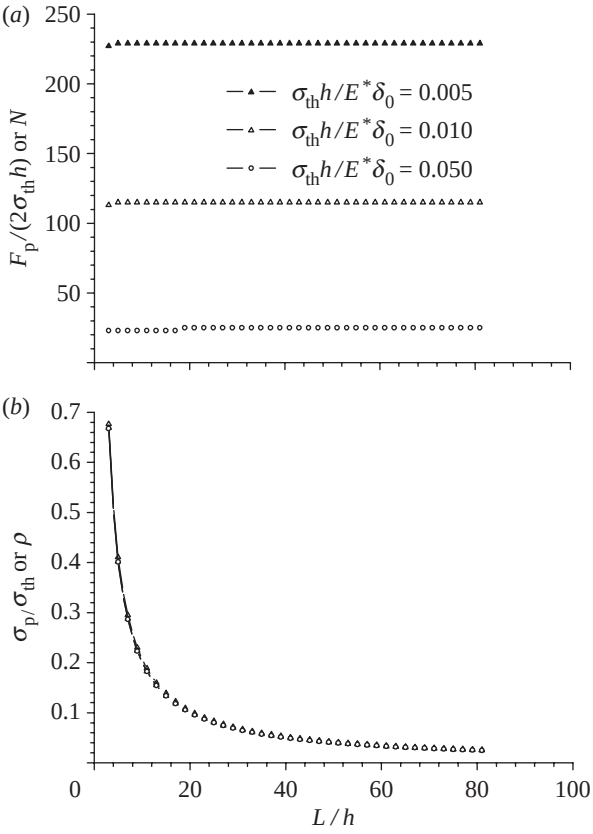

Figure 8. (*a*) The normalized pull-off force $F_{\mathrm{p}}/(2\sigma_{\mathrm{th}}h)$ or the critical number of rigid plates N as a function of the normalized space L/h and (*b*) plots of the normalized pull-off stress $\sigma_{\mathrm{p}}/\sigma_{\mathrm{th}}$ via the normalized space L/h to satisfy ELS and flaw insensitivity for the plane-strain model shown in figure 2.

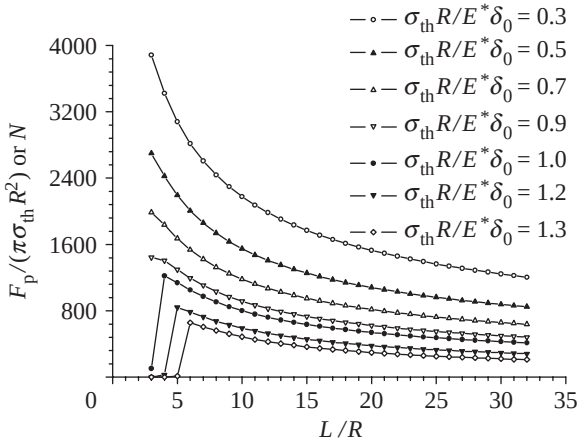

Figure 9. The normalized pull-off force $F_p/(\pi\sigma_{th}R^2)$ or the critical number of fibres N as a function of the normalized space L/R to satisfy ELS and flaw insensitivity in the adhesive contact model of fibrillar structure with fibrils in line array distributions.

4.2. Three-dimensional fibrillar interface contact

4.2.1. Line array pattern. In the case of adhesive contact between an elastic substrate and a rigid fibrillar structure with fibrils distributing in a line array, one can see that the normalized pull-off force $F_p/(\pi\sigma_{th}R^2)$ is equal to the critical number N quantitatively in equation (3.14). Figure 9 shows the normalized pull-off force $F_p/(\pi\sigma_{th}R^2)$ and the critical number of fibres N as a function of the normalized space of neighbouring fibres L/R for several different values of $\sigma_{th}R/E^*\delta_0$ to satisfy the conditions of ELS and flaw insensitivity. From figure 9, one can see that the pull-off force and the critical number of fibrils are influenced significantly by the non-dimensional parameters $\sigma_{th}R/E^*\delta_0$ and L/R. For a determined L/R, the pull-off force and the critical number increase when the parameter $\sigma_{th}R/E^*\delta_0$ decreases. For a smaller value of $\sigma_{th}R/E^*\delta_0$, the pull-off force $F_p/(\pi\sigma_{th}R^2)$ and the critical number N will decrease smoothly with an increasing value of L/R. For a larger value of $\sigma_{th}R/E^*\delta_0$, the pull-off force and the critical number will increase first along with L/R and then decrease, which means that the pull-off force can obtain a maximum value at an optimal L/R in the case with a larger $\sigma_{th}R/E^*\delta_0$. The pull-off stress will decrease along with increasing space L/R and the curve looks like that in figure 8*b*.

4.2.2. Hexagonal lattice pattern. According to equations (3.20)–(3.22), the normalized pull-off force and the critical number N as a function of the normalized space L/R to satisfy ELS and flaw-insensitivity conditions are shown in figure 10 with fibrils distributing in a hexagonal lattice pattern. From figure 10, one can see that for a determined parameter $\sigma_{th}R/E^*\delta_0$, the normalized pull-off force increases first with the increasing normalized space L/R and then decreases for larger L/R. There exists a certain value of L/R in each case, at which the pull-off force and the critical number N attain maximum. For a fixed space L/R, the pull-off force and N are always increasing along with the

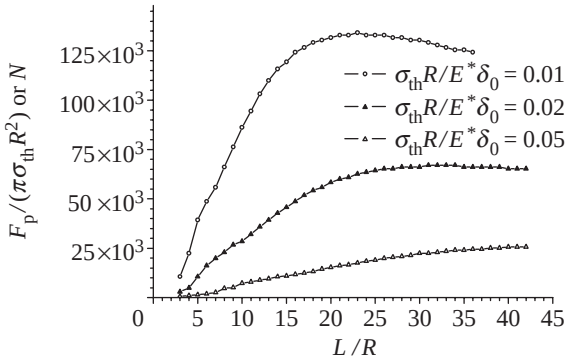

Figure 10. The normalized pull-off force $F_p/(\pi\sigma_{th}R^2)$ or the critical number of fibres N as a function of the normalized space L/R to satisfy ELS and flaw insensitivity in the adhesive contact model of fibrillar structure with fibrils in hexagonal lattice distributions.

decreasing parameter $\sigma_{th}R/E^*\delta_0$. As for the pull-off stress, it will decrease along with the increasing space L/R, which looks like the curve in figure 8*b*.

4.2.3. Square lattice pattern. Figure 11*a*,*b* plots the curves of the normalized pull-off force (the critical number N) via the normalized space of neighbouring fibrils L/R to satisfy the ELS and flaw-insensitivity conditions in adhesive contact of fibrillar interface with fibrils distributing in a square lattice pattern. Owing to large difference between the quantities of the normalized pull-off force for different values of $\sigma_{th}R/E^*\delta_0$, we plot the relations in two figures (figure 11*a*,*b*) to make the curves more clear. From the two figures, one can see that the relation between the normalized pull-off force (the critical number N) and the ratio L/R is much more complex than that in the former cases for a given $\sigma_{th}R/E^*\delta_0$. For smaller non-dimensional value $\sigma_{th}R/E^*\delta_0$, the normalized pull-off force will increase first with the increasing ratio L/R, then decrease quickly after achieving a maximum value, from which one can see that the pull-off force is influenced significantly by tuning the geometrical parameter of fibrillar structures so that it is convenient to choose the space between neighbouring fibrils to obtain the required adhesion properties. When the value of $\sigma_{th}R/E^*\delta_0$ increases, the relation between the normalized pull-off force and L/R consists of four regimes along with an increasing L/R: (i) the pull-off force (or the critical number N) increases at the initial stage, (ii) decreases at certain value of L/R, (iii) then increases again to a second top value, and (iv) after that, decreases once again. For a fixed ratio L/R, the pull-off force is always larger for a smaller $\sigma_{th}R/E^*\delta_0$. From the above, one can see that the pull-off force can be regulated by tuning the geometrical parameter of fibrillar structures. Furthermore, one can find easily that the effective adhesion strength (pull-off stress) decreases and asymptotically approaches zero with the increasing ratio L/R, and this variation looks very similar to that in figure 8*b*.

5. DISCUSSION

In this paper, we study only the cases of rigid fibrillar structures in contact with elastic substrates to satisfy the ELS and flaw insensitivity, from which the pull-off

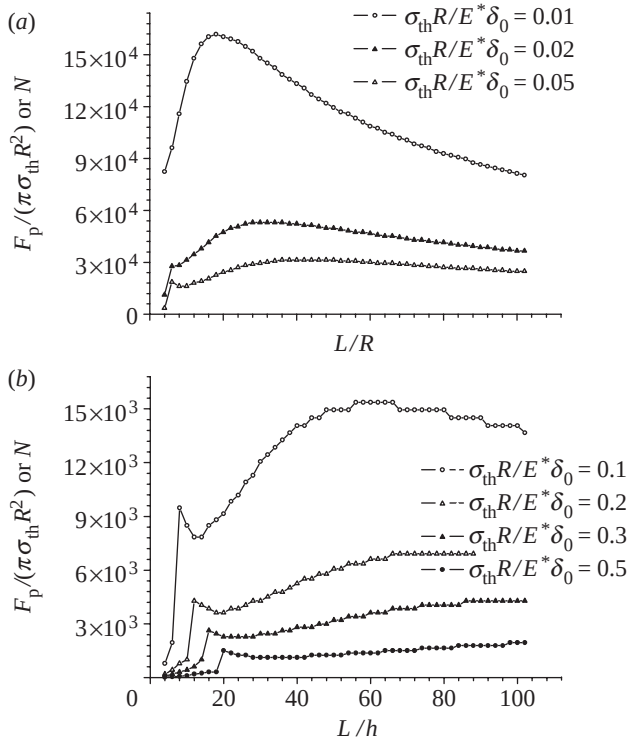

Figure 11. The normalized pull-off force $F_p/(\pi\sigma_{th}R^2)$ or the critical number of fibres N as a function of the normalized space L/R for (*a*) three smaller non-dimensional parameters $\sigma_{th}R/E^*\delta_0$=0.01, 0.03 and 0.05 and (*b*) four larger non-dimensional parameters $\sigma_{th}R/E^*\delta_0$=0.1, 0.2, 0.3 and 0.5 to satisfy ELS and flaw insensitivity in the adhesive contact model of fibrillar structure with fibrils in square lattice distributions.

force, the effective adhesion strength and the critical number of fibrils are influenced significantly by tuning the geometrical parameters of fibrillar structures. We can find an optimal space of neighbouring fibrils to achieve maximum pull-off force. The critical number of fibres is a criterion to justify whether the equation $P = NF$ can be used correctly in studying periodical structures. For a determined space of neighbouring fibrils and the size of single fibril not larger than the critical one, if the number of fibrils N^* is larger than the critical number N, ELS assumption cannot be used any more and the idea of 'contact splitting' to increase the adhesion force becomes unsuitable. On the contrary, if $N^* \leq N$, it is reasonable and very convenient to use ELS to analyse the adhesion characters of fibrillar structures.

From the analysis in this paper, one can see that if the number of fibrils satisfies ELS and flaw-insensitivity conditions, it needs only to tune the geometrical parameters to enhance adhesion.

As for the case of elastic fibrillar structures in contact with elastic or rigid substrates, Hui *et al.* (2004) has investigated this problem to some extent, in which they suppose that the pull-off of a fibril can be viewed as the growth of a pre-existing crack for the case of rigid fibrils in contact with substrates; however, this does not apply to an elastic fibril since the exterior of an elastic fibril is not an external crack. Details can be found in Hui *et al.* (2004). Yao & Gao (2006) have investigated the hierarchical fibrillar structures and made a comparison between their results and the observed hierarchical structure of the gecko. For cases of elastic fibrils, the elastic strain energy stored in any fibril should be considered in addition to the energy creating new surfaces during pull-off. Are there any constraints on the number of elastic fibrils and what effect will be produced on the pull-off force and adhesion strength? This more realistic mechanical mechanism adopted by bioadhesion systems will be left to future work.

The work reported here was supported by NSFC (10672165) and KJCX2-YW-M04.

REFERENCES

Arzt, E., Gorb, S. & Spolenak, R. 2003 From micro to nano contacts in biological attachment devices. *Proc. Natl Acad. Sci. USA* **100**, 10 603–10 606. (doi:10.1073/pnas.1534701100)

Autumn, K., Liang, Y. C., Hsieh, S. T., Zesch, W., Chan, W. P., Kenny, T. W., Fearing, R. & Full, R. J. 2000 Adhesion forces of a single gecko foot-hair. *Nature* **405**, 681–685. (doi:10.1038/35015073)

Autumn, K. *et al.* 2002 Evidence for van der Waals adhesion in gecko setae. *Proc. Natl Acad. Sci. USA* **99**, 12 252–12 256. (doi:10.1073/pnas.192252799)

Baney, J. M. & Hui, C. Y. 1997 A cohesive zone model for the adhesion of cylinders. *J. Adhes. Sci. Technol.* **11**, 393–406.

Barenblatt, G. I. 1985 *The mathematical theory of equilibrium cracks in brittle fracture.* Advances in applied mechanics, vol. VII, pp. 55–129. New York, NY: Academic Press.

Barquins, M. 1988 Adherence and rolling kinetics of a rigid cylinder in contact with a natural rubber surface. *J. Adhesion* **26**, 1–12.

Barthel, E. 1998 On the description of the adhesive contact of spheres with arbitrary interaction potentials. *J. Coll. Interface Sci.* **200**, 7–18. (doi:10.1006/jcis.1997.5309)

Carpick, R. W., Agrait, N., Ogletree, D. F. & Salmeron, M. 1996 Variation of the interfacial shear strength and adhesion of a nanometer sized contact. *Langmuir* **12**, 3334–3340. (doi:10.1021/la9509007)

Chaudhury, M. K., Weaver, T., Hui, C. Y. & Kramer, E. J. 1996 Adhesion contact of cylindrical lens and a flat sheet. *J. Appl. Phys.* **80**, 30–37. (doi:10.1063/1.362819)

Chen, S. & Gao, H. 2006*a* Non-slipping adhesive contact of an elastic cylinder on stretched substrates. *Proc. R. Soc. A* **462**, 211–228. (doi:10.1098/rspa.2005.1553)

Chen, S. & Gao, H. 2006*b* Generalized Maugis–Dugdale model of an elastic cylinder in non-slipping adhesive contact with a stretched substrate. *Int. J. Mater. Res.* **97**, 584–593.

Chen, S. & Gao, H. 2006*c* Non-slipping adhesive contact between mismatched elastic spheres: a model of adhesion mediated deformation sensor. *J. Mech. Phys. Solids* **54**, 1548–1567. (doi:10.1016/j.jmps.2006.03.001)

Chen, S. & Gao, H. 2007 Bio-inspired mechanics of reversible adhesion: orientation-dependent adhesion strength for non-slipping adhesive contact with transversely isotropic elastic materials. *J. Mech. Phys. Solids* **55**, 1001–1015. (doi:10.1016/j.jmps.2006.10.008)

Chen, S. & Wang, T. C. 2006 General solution to two-dimensional nonslipping JKR model with a pulling force in an arbitrary direction. *J. Coll. Interface Sci.* **302**, 363–369. (doi:10.1016/j.jcis.2006.06.014)

Derjaguin, B. V., Muller, V. M. & Toporov, Y. P. 1975 Effect of contact deformations on the adhesion of particles. *J. Coll. Interface Sci.* **53**, 314–326. (doi:10.1016/0021-9797(75)90018-1)

Dugdale, D. S. 1960 Yielding of steel sheets containing slits. *J. Mech. Phys. Solids* **8**, 100–104. (doi:10.1016/0022-5096(60)90013-2)

Gao, H. 2006 Application of fracture mechanics concepts to hierarchical biomechanics of bone and bone-like materials. *Int. J. Fract.* **138**, 101–137. (doi:10.1007/s10704-006-7156-4)

Gao, H. & Chen, S. 2005 Flaw insensitivity in a thin strip under tension. *J. Appl. Mech.* **72**, 732–737. (doi:10.1115/1.1988348)

Gao, H. & Yao, H. 2004 Shape insensitive optimal adhesion of nanoscale fibrillar structures. *Proc. Natl Acad. Sci. USA* **101**, 7851–7856. (doi:10.1073/pnas.0400757101)

Gao, H., Ji, B., Jäger, I. L., Arzt, E. & Fratzl, P. 2003 Materials become insensitive to flaws at nanoscale: lessons from nature. *Proc. Natl Acad. Sci. USA* **100**, 5597–5600. (doi:10.1073/pnas.0631609100)

Gao, H., Wang, X., Yao, H., Gorb, S. & Arzt, E. 2005 Mechanics of hierarchical adhesion structures of gecko. *Mech. Mater.* **37**, 275–285. (doi:10.1016/j.mechmat.2004.03.008)

Geim, A. K. *et al.* 2003 Microfabricated adhesive mimicking gecko foot-hair. *Nat. Mater.* **2**, 461–463. (doi:10.1038/nmat917)

Glassmaker, N. J., Jagota, A., Hui, C. Y. & Kim, J. 2004 Design of biomimetic fibrillar interface: 1. Making contact. *J. R. Soc. Interface* **1**, 23–33. (doi:10.1098/rsif.2004.0004)

Gorb, S. & Scherge, M. 2000 Biological microtribology: anisotropy in frictional forces of orthopteran attachment pads reflects the ultrastrucutre of a highly deformable material. *Proc. R. Soc. B* **267**, 1239–1244. (doi:10.1098/rspb.2000.1133)

Greenwood, J. A. & Johnson, K. L. 1981 The mechanics of adhesion of viscoelastic solids. *Philos. Mag.* **43**, 697–711.

Greenwood, J. A. & Johnson, K. L. 1998 An alterative to the Maugis model of adhesion between elastic spheres. *J. Phys. D: Appl. Phys.* **31**, 3279–3290. (doi:10.1088/0022-3727/31/22/017)

Hodges, C. S., Looi, L., Cleaver, J. A. S. & Ghadiri, M. 2004 Use of the JKR model for calculating adhesion between rough surfaces. *Langmuir* **20**, 9571–9576. (doi:10.1021/la035790f)

Huber, G., Gorb, S., Spolenak, R. & Artz, E. 2005 Resolving the nanoscale adhesion of individual gecko spatulae by atomic force microscopy. *Biol. Lett.* **1**, 2–4. (doi:10.1098/rsbl.2004.0254)

Hui, C. Y., Lin, Y. Y., Baney, J. M. & Kramer, E. J. 2001 The mechanics of contact and adhesion of periodically rough surfaces. *J. Polym. Sci. B: Polym. Phys.* **39**, 1195–1214. (doi:10.1002/polb.1094)

Hui, C. Y., Jagota, A., Lin, Y. Y. & Kramer, E. J. 2002 Constraints on microcontact printing imposed by stamp deformation. *Langmuir* **18**, 1394–1407. (doi:10.1021/la0113567)

Hui, C. Y., Glassmaker, N. J., Tang, T. & Jagota, A. 2004 Design of biomimetic fibrillar interface: 2. Mechanics of enhanced adhesion. *J. R. Soc. Interface* **1**, 35–48. (doi:10.1098/rsif.2004.0005)

Johnson, K. L. 1985 *Contact mechanics*. Cambridge, UK: Cambridge University Press.

Johnson, K. L. & Greenwood, J. A. 1997 An adhesion map for the contact of elastic spheres. *J. Coll. Interface Sci.* **192**, 326–333. (doi:10.1006/jcis.1997.4984)

Johnson, K. L., Kendall, K. & Roberts, A. D. 1971 Surface energy and the contact of elastic solids. *Proc. R. Soc. A* **324**, 301–313. (doi:10.1098/rspa.1971.0141)

Kesel, A. B., Martin, A. & Seidl, T. 2003 Adhesion measurements on the attachment devices of the jumping spider *Evarcha arcuata*. *J. Exp. Biol.* **206**, 2733–2738. (doi:10.1242/jeb.00478)

Kim, K. S., McMeeking, R. M. & Johnson, K. L. 1998 Adhesion, slip cohesive zone and energy fluxes for elastic spheres in contact. *J. Mech. Phys. Solids* **46**, 243–266. (doi:10.1016/S0022-5096(97)00070-7)

Maugis, D. J. 1992 Adhesion of spheres: the JKR–DMT transition using a Dugdale model. *J. Coll. Interface Sci.* **150**, 243–269. (doi:10.1016/0021-9797(92)90285-T)

Meine, K., Klob, K., Schneider, T. & Spaltmann, D. 2004 The influence of surface roughness on the adhesion force. *Surf. Interface Anal.* **36**, 694–697. (doi:10.1002/sia.1738)

Morrow, C., Lovell, M. & Ning, X. 2003 A JKR–DMT transition solution for adhesive rough surface contact. *J. Phys. D: Appl. Phys.* **36**, 534–540. (doi:10.1088/0022-3727/36/5/317)

Muller, V. M., Yushenko, V. S. & Derjaguin, B. V. 1980 On the influence of molecular forces on the deformation of an elastic sphere and its sticking to s rigid contact. *J. Coll. Interface Sci.* **77**, 91–101. (doi:10.1016/0021-9797(80)90419-1)

Niederegger, S., Gorb, S. & Jiao, Y. 2002 Contact behavior of tenent setae in attachment pads of the blowfly *Calliphota vivina* (Diptera, Calliphoridae). *J. Comp. Physiol A* **187**, 961–970. (doi:10.1007/s00359-001-0265-7)

Persson, B. N. J. 2003 On the mechanism of adhesion in biological systems. *J. Chem. Phys.* **118**, 7614–7621. (doi:10.1063/1.1562192)

Robbe-Valloire, F. & Barquins, M. 1998 Adhesive contact and kinetics of adherence between a rigid cylinder and an elastomeric solid. *Int. J. Adhesion Adhesives* **18**, 29–34. (doi:10.1016/S0143-7496(97)00064-X)

Roberts, A. D. & Thomas, A. G. 1975 The adhesion and friction of smooth rubber surfaces. *Wear* **33**, 45–64. (doi:10.1016/0043-1648(75)90223-9)

Russell, A. P. 2002 Integrative functional morphology of the *gekkotan* adhesion system (Reptilia: *Gekkota*). *Integr. Comp. Biol.* **42**, 1154–1163. (doi:10.1093/icb/42.6.1154)

Schwarz, U. D. 2003 A generalized analytical model for the elastic deformation of an adhesive contact between a sphere and a flat surface. *J. Coll. Interface Sci.* **261**, 99–106. (doi:10.1016/S0021-9797(03)00049-3)

Spolenak, R., Gorb, S., Gao, H. & Artz, E. 2005 Effects of contact shape on the scaling of biological attachments. *Proc. R. Soc. A* **461**, 305–319. (doi:10.1098/rspa.2004.1326)

Tang, T., Hui, C. Y. & Glassmaker, N. J. 2005 Can a fibrillar interface be stronger and tougher than a non-fibrillar one? *J. R. Soc. Interface* **2**, 505–516. (doi:10.1098/rsif.2005.0070)

Yao, H. & Gao, H. 2006 Bio-inspired mechanics of robust and releasable adhesion on rough surface. *J. Mech. Phys. Solids* **54**, 1120–1146. (doi:10.1016/j.jmps.2006.01.002)

NOTICE OF CORRECTION

The name of the second author is now correct.

9 August 2007

JOURNAL OF THE ROYAL SOCIETY Interface
JOURNAL OF THE ROYAL SOCIETY Interface